

Electrokinetic stringency control in self-assembled monolayer-based biosensors for multiplex urinary tract infection diagnosis

Tingting Liu, MS^a, Mandy L.Y. Sin, PhD^{a,b}, Jeff D. Pyne, BS^a, Vincent Gau, PhD^c, Joseph C. Liao, MD^{b,d}, Pak Kin Wong, PhD^{a,*}

^aDepartment of Aerospace and Mechanical Engineering, University of Arizona, Tucson, AZ, USA

^bDepartment of Urology, Stanford University, Stanford, CA, USA

^cGeneFluidics Inc., Irwindale, CA, USA

^dVeterans Affairs Palo Alto Health Care System, Palo Alto, CA, USA

Received 1 March 2013; accepted 5 July 2013

Abstract

Rapid detection of bacterial pathogens is critical toward judicious management of infectious diseases. Herein, we demonstrate an in situ electrokinetic stringency control approach for a self-assembled monolayer-based electrochemical biosensor toward urinary tract infection diagnosis. The in situ electrokinetic stringency control technique generates Joule heating induced temperature rise and electrothermal fluid motion directly on the sensor to improve its performance for detecting bacterial 16S rRNA, a phylogenetic biomarker. The dependence of the hybridization efficiency reveals that in situ electrokinetic stringency control is capable of discriminating single-base mismatches. With electrokinetic stringency control, the background noise due to the matrix effects of clinical urine samples can be reduced by 60%. The applicability of the system is demonstrated by multiplex detection of three uropathogenic clinical isolates with similar 16S rRNA sequences. The results demonstrate that electrokinetic stringency control can significantly improve the signal-to-noise ratio of the biosensor for multiplex urinary tract infection diagnosis.

From the Clinical Editor: Urinary tract infections remain a significant cause of mortality and morbidity as secondary conditions often related to chronic diseases or to immunosuppression. Rapid and sensitive identification of the causative organisms is critical in the appropriate management of this condition. These investigators demonstrate an in situ electrokinetic stringency control approach for a self-assembled monolayer-based electrochemical biosensor toward urinary tract infection diagnosis, establishing that such an approach significantly improves the biosensor's signal-to-noise ratio.

© 2014 Elsevier Inc. All rights reserved.

Key words: Urinary tract infection; Stringency control; Multiplex detection; Matrix effects; Self-assembled monolayers

Infectious diseases caused by bacterial pathogens are common causes of patient morbidity and a major global healthcare challenge.¹ For instance, urinary tract infection (UTI), the most common bacterial infection of any organ system, is a major cause of health care expenditures, accounting for millions of office visits and hospital admissions every year in America.^{2,3} To properly manage infectious diseases, patient samples, such as urine and blood, are delivered to clinical microbiology laboratories for pathogen identification. A major limitation of the standard culture-based diagnostic approach,

however, is that at least two to three days is required from specimen collection to result reporting. The long delay is a result of sample transport to the clinical microbiology laboratory and overnight culture. Without direct information about the pathogens, antibiotic treatments are typically chosen based on the worst-case scenario assumption, even in situations where bacteria pathogens are ultimately found not to be the culprit. Therefore, a biosensor that allows rapid identification of the pathogens at the point of care will be tremendously beneficial to the management and treatment of infectious diseases.

Recently, numerous molecular and nanoengineered pathogen detection strategies have been developed.^{4,5} Self-assembled monolayer (SAM)-based electrochemical biosensors, in particular, have received a lot of attention in the point-of-care diagnostics community.^{6–11} Electrochemical nucleic acid biosensors have several advantages over other detection methods. These advantages include cost-effectiveness, excellent

This work is supported by National Institutes of Health, Health Director's New Innovator Award (1DP2OD007161-01), NIAID (1U01AI082457-01 and 2R44AI088756-03), and NSF (0930900; 0900899).

*Corresponding author: Aerospace and Mechanical Engineering, University of Arizona, Tucson, AZ 85721, USA.

E-mail address: pak@email.arizona.edu (P.K. Wong).

1549-9634/\$ – see front matter © 2014 Elsevier Inc. All rights reserved.
<http://dx.doi.org/10.1016/j.nano.2013.07.006>

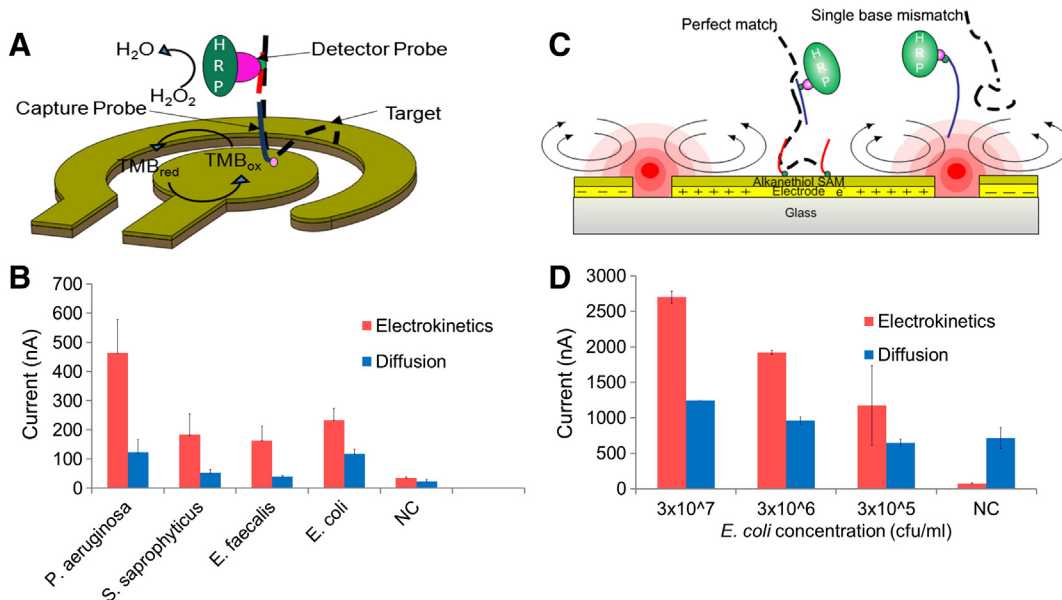


Figure 1. (A) Self-assembled monolayer based electrochemical pathogen sensor. (B) Non-specific binding is removed by the temperature rise and fluid flow for washing based on electrokinetic control. (C) *Pseudomonas aeruginosa*, *Staphylococcus saprophyticus*, *Enterococcus faecalis*, and *Escherichia coli* are detected in the conditions of diffusion and electrokinetics. (D) The concentration of *E. coli* was measured with respect to diffusion and electrokinetics. A square wave with voltage of 6 Vpp at 200 kHz was applied for 8 minutes.

sensitivity and specificity, compatibility with micro/nano fabrication technology, and the availability of compact and portable electronic interfaces. For instance, a SAM-based electrochemical biosensor array for detecting species-specific bacterial 16S rRNA has been reported for rapid UTI diagnosis.^{12–14} In the “sandwich”-binding scheme of the biosensor, the target 16S rRNA is anchored at the sensor surface by a DNA capture probe and is also hybridized to a DNA detector probe. The detector probe is labeled with a reporter coupled to an oxidoreductase enzyme, which interacts with the substrate and generates a redox signal to be detected by the sensor electrodes (Figure 1, A). While electrochemical biosensor is a promising platform for rapid diagnosis of infectious diseases, several technological challenges remain for point-of-care applications. In clinical samples, such as blood and urine, matrix components including metabolites, proteins, and salts can introduce non-specific binding, which reduces the overall sensitivity of the assay and may lead to false positives.¹⁵ Furthermore, bacterial pathogens may share similar nucleic acid sequences that can reduce the diagnostic accuracy of the molecular assay. While it is possible to design highly specific capture and detector probe pairs for each species, multiplex detection with multiple detector probes simultaneously can introduce crosstalk between different sensors.^{16–21} The crosstalk may lead to non-specific detection of the bacterial species and can result in an overestimation of the target concentration. Within a clinical context, it is essential to reduce the uncertainty due to non-specific binding and improve the overall reliability of the multiplex pathogen identification assays.

Innovative technologies for stringency control are highly desirable to address the aforementioned issues toward multiplex detection of infectious diseases. Stringency control by adjusting the hybridization temperature and stringency wash has been

widely adopted to remove non-specific binding in hybridization assays.^{22–26} However, these strategies could be challenging to implement in resource-limited settings. In this study, we exploit alternating current (AC) electrokinetics to generate local heating and fluid motion for in situ electrokinetic stringency control. AC electrokinetics requires only simple electronic interfaces and a low driving voltage, which eliminates the need for a high driving voltage power supply and avoids bubble formation due to electrolysis. These characteristics render AC electrokinetics a promising platform for point-of-care diagnostics.²⁷

For stringency control, an applied electric field can create a Joule heating induced temperature elevation, which is a result of the Joule heating as electric current flows through the conductive hybridization buffer.²⁸ The electrical conductivity of the fluid and the amplitude of the electric field can control the magnitude of the temperature rise. Depending on the electrode configuration, the local heating can also generate a spatial temperature distribution, which induces gradients of conductivity and permittivity. The interaction between these gradients and the electric field can create electrokinetic forces and bulk electrothermal fluid motion. The temperature distribution at equilibrium can be determined by considering the simplified energy equation:^{29–32}

$$k \nabla^2 T + \sigma E^2 = 0$$

where T is the temperature of the medium, σ is the conductivity of the medium, k is the thermal diffusivity, and E is the electric field. For a pair of parallel electrodes with a small gap, the temperature rise near the gap of the electrodes has been estimated to be:

$$\Delta T = \sigma V_{rms}^2 / 8k$$

where V_{rms} is the root mean square voltage. An analytical expression for the order of magnitude of the electrohydrodynamic force has been derived:^{30,31}

$$f_{ACEF} = -M(\omega, T) \left(\frac{\varepsilon \sigma V_{rms}^4}{2k\pi^3 r^3 T} \right) \left(1 - \frac{2\theta}{\pi} \right)$$

$$M(\omega, T) = \left(\frac{\frac{T}{\sigma} \left(\frac{\partial}{\partial T} \right) - \frac{T}{\varepsilon} \left(\frac{\partial \varepsilon}{\partial T} \right)}{1 + (\omega\tau)^2} + \frac{T}{2\varepsilon} \left(\frac{\partial \varepsilon}{\partial T} \right) \right)$$

where r and θ are the polar coordinates with reference to the middle of the electrode gap, $M(\omega, T)$ is a dimensionless factor describing the variation of the electrothermal force as a function of both frequency and temperature, and τ is the charge relaxation time. These equations characterize the temperature rise and the electrothermal force. Previously, we had characterized the electrothermal fluid motion³², and an *in situ* electrokinetic technique had been developed for signal enhancement.¹² The fluid motion and local temperature rise may potentially be applied to increase the hybridization stringency and remove non-specific binding. Previous studies have also demonstrated the use of external electric fields for electrically removing non-specific targets in optical DNA sensors.^{33,34} However, the combination of electrothermal flow and Joule heating induced temperature rise has not been explored for electrokinetic stringency control. Furthermore, *in situ* electrokinetic stringency control has not been applied directly on SAM-based electrochemical sensors for multiplex pathogen detection despite its potential in point-of-care diagnostics.

In this study, we describe an *in situ* electrokinetic stringency control technique by utilizing AC electrothermal fluid motion and the Joule heating effect to remove non-specific binding and to improve the specificity of the electrochemical nucleic acid biosensor. Joule heating is applied to induce a high stringency that only permits highly homologous sequences to bind, and the electrothermal fluid motion is utilized to remove non-specific binding similar to a stringent wash in DNA hybridization (Figure 1, B). Single nucleotide mismatch discrimination with electrokinetic stringency control is investigated using synthetic oligonucleotides with the electrochemical biosensor. The background level due to the matrix effects of clinical urine samples is also estimated as a function of the applied voltage. To explore the clinical utility of the electrokinetic stringency control technique, multiplex detection of uropathogenic clinical isolates with similar 16S rRNA sequences is investigated using multiple detection probes simultaneously.

Methods

Reagents and samples

Oligonucleotide probes and synthetic DNA targets were obtained from Integrated DNA Technologies (Coralville, IA). The *E. coli* capture probe and detector probe are 24 base pairs in length, which are modified with 5' biotin and 3' fluorescein, respectively (Table 1). The perfect match target is complementary to the *E. coli* capture and detector probes, and the single-

Table 1
Sequences of probes and oligonucleotides.

Probe and oligonucleotide	Sequence
<i>Escherichia coli</i>	5' CTG CGG GTA ACG TCA ATG AGC AAA 3'
Capture (EC471C)	5' GGT ATT AAC TTT ACT CCC TTC CTC 3'
Detector (EC447D)	
<i>Proteus mirabilis</i>	5' AGC GTT CCC GAA GGC ACT CCT C 3'
Capture (PM1019C)	5' TAT CTC TAA AGG ATT CGC TGG A 3'
Detector (PM997D)	
<i>Pseudomonas aeruginosa</i>	5' CCC GGG GAT TTC ACA TCC AAC TT 3'
Capture (PA594C)	5' GCT GAA CCA CCT ACG CGC GCT TT 3'
Detector (PA570D)	
Universal bacterial	5' TCG TTT ACR GCG TGG ACT ACC A 3'
Capture (UNI798C)	5' GGG TAT CTA ATC CTG TTT GCT C 3'
Detector (UNI776D)	
<i>Enterococcus spp.</i>	5' ACC GCG GGT CCA TCC ATC AG 3'
Capture (EF220C)	5' CGA CAC CCG AAA GCG CCT TT 3'
Detector (EF200D)	
<i>Enterobacteriaceae</i>	5' ACT TTA TGA GGT CCG CTT GCT CT 3'
Capture (EB1275C)	5' CGC GAG GTC GCC TTC CTT TGT AT 3'
Detector (EB1252D)	
Perfect match	5' ATG AAG AAG GCC TTC GGG TTG TAA AGT ACT TTC AC GGG GAG GAA GG AGT AAA GTT AAT ACC TTT GCT CAT TGA C 3'
Single base mismatch	5' ATG AAG AAG GCC TTC GGG TTG TAA AGT ACT TTC AC GGG GAG GAA GG AGT AAA GTT AAT ACC TTT ACT CAT TGA C 3'

base mismatch target has a mismatch nucleotide with the capture probe. Uropathogenic isolates including *Pseudomonas aeruginosa* (*P. aeruginosa*), *Proteus mirabilis* (*P. mirabilis*), *Staphylococcus saprophyticus* (*S. saprophyticus*), *Enterococcus faecalis* (*E. faecalis*) and *Escherichia coli* (*E. coli*) as well as clinical urine samples were obtained from the clinical microbiology laboratory at the Veterans Affairs Palo Alto Health Care System (VAPAHCS). Before the experiment, the bacterial colonies were freshly incubated in Luria broth (LB) and grown to logarithmic phase.

Electrochemical sensor array

The electrochemical sensor electrodes were fabricated on glass substrates by photolithography. A 25 nm thick titanium and a 125 nm thick gold electrode were evaporated on patterned photoresist structures. The electrodes were patterned by lift-off. The sensor arrays were cleaned by isopropanol and deionized water before coating with self-assembled monolayers for immobilizing the appropriate capture probes and minimizing non-specific bindings. Each sensor was immobilized with a biotinylated-capture probe.¹³ A plastic well manifold fabricated by a laser machining system (Universal Laser System Inc. VLS2.30) was bonded to the sensor array. The electrical signal was supplied by a function generator (HP33120A) and monitored by a digital oscilloscope (GW Instek GDS-1102). The sensor array was connected to a multi-channel potentiostat (GeneFluidics) for amperometric reading.

Electrochemical assay for bacterial 16S rRNA

A schematic overview of the detection strategy of the electrochemical sensor array is shown in Figure 1, A.

Specifically, 20 μl of the bacterial sample was mixed with 12 μl of 10 mg/ml lysozyme in 4 mM EDTA, 40 mM Tris–HCl of pH 8.0, and 0.2% Triton X-100. The mixture was incubated at room temperature for 5 minutes. The sample was then mixed with 8 μl of 1 M NaOH and followed by additional incubation for 5 minutes at room temperature. Sixty μl of detector probe (0.5 μM) in 2.5% bovine serum albumin (BSA) (Sigma, St. Louis, MO) and 1 M phosphate buffer of pH 7.4, was added to the bacterial lysate and incubated at 37 C for 10 minutes to allow the hybridization between the bacterial 16S rRNA and the detector probe. Fifty μl of bacterial lysate-detector mixture was loaded on the well, and the incubation proceeded for 10 minutes at room temperature with and without electrokinetic stringency control. After the mixture was washed and the sensor was dried, 6 μl of 0.5 U/ml anti-fluorescein horseradish peroxidase (HRP) Fab fragments (Roche Diagnostics) in 1 M phosphate buffer saline containing 0.5% casein was added on the sensor and incubated at room temperature for 15 minutes. After washing and drying, the sensor was loaded onto the potentiostat (GeneFluidics). The amperometric currents were taken for all 16 sensors by applying voltage of -200 mV, at 60s when the HRP redox reaction reached steady state. For detecting single-base mismatches, this lysing process was substituted with a 10 minutes incubation of 10 μl of 100 nM synthetic target and 90 μl of 500 nM detector probe.

Multiplex detection

For multiplex detection, a cocktail of six different detector probes, including universal bacterial probe (UNI776D), *Enterobacteriaceae* probe (EB1252D), *Escherichia coli* probe (EC447D), *Proteus mirabilis* probe (PM997D), *Pseudomonas aeruginosa* probe (PA570D), and *Enterococcus faecalis* probe (EF200D) (defined in Table 1), was diluted into 1 M phosphate buffer with 2.5% BSA buffer. The detector probe cocktail was mixed with the bacterial lysate and incubated at 37 °C for 5 minutes. The mixture was loaded on the pre-coated sensors with *E. coli*, *P. mirabilis*, and *P. aeruginosa* capture probes immobilized. Negative controls that apply the same procedures including capture probe and cocktail detector probe without bacteria were also tested on the capture probe pre-coated sensors. For electrokinetic stringency control a square wave with 6 V peak-to-peak (Vpp) at 200 kHz was applied to the sample with conductivity of 6.7 S/m for 8 minutes.

Micro-scale thermometry experiments

To characterize the temperature rise,^{35,36} two fluorescent dyes, Rhodamine B (RhB) and Rhodamine 110 (Rh110), were used for dual-color fluorescence thermometry. RhB is a temperature-dependent fluorescent dye and its intensity decreases linearly with the temperature. Rh110 is a temperature-independent dye for normalizing the intensity data. Calibration was performed using the hybridization buffer premixed with RhB and Rh110. The chamber was sealed and mounted under a temperature control water bath. The temperature of the water bath was measured by a thermocouple (LINI-T, UT33C) and recorded as the reference temperature. Fluorescence images were captured at each reference temperature. The intensity values were

normalized via the intensity value at room temperature to obtain the calibration curve. The temperature measurement was performed at different applied voltages to obtain the voltage-temperature relationship. The temperature in steady state was used to calculate the melting curve for the single-base mismatch detection experiment.

Nearest-neighbor model based melting analysis

The nearest-neighbor model was used to estimate the melting curves.³⁷ Based on the nearest-neighbor model, the energetic stability of a given base pair depends on the identity and orientation of neighboring base pairs. The fraction of nucleic acids hybridized as a function of the equilibrium constant K can be calculated as:³⁸

$$\alpha = \frac{1 + C_T K - \sqrt{1 + 2C_T K}}{C_T K}$$

where C_T is the total concentration of nucleic acid strands in the solution.

The equilibrium constant can be estimated by Van't Hoff equation:

$$K = \exp\left(-\frac{\Delta H^0}{RT} + \frac{\Delta S^0}{R}\right)$$

where ΔH^0 is the change in enthalpy, ΔS^0 is the change in entropy, T is temperature, and R is the gas constant.

Results

Electrochemical biosensor for bacterial 16S rRNA

The electrochemical sensor for bacterial 16S rRNA was applied to identify and quantify uropathogens by measuring the redox signal. Figure 1, C shows detection of four common uropathogens with and without electrokinetics. With the appropriate capture and detector probes, the electrochemical sensor selectively detected the bacteria. By applying electrokinetics directly on the sensor electrodes, the signal-to-noise ratio increased for all uropathogens, which improved the overall sensitivity of the SAM-based electrochemical biosensor array. The magnitude of the electrical current was observed to be proportional to the concentration of the bacteria with and without electrokinetics (Figure 1, D). These results demonstrate the SAM-based electrochemical assay is applicable for detecting uropathogens, and electrokinetics can be applied for enhancing the sensitivity of the sensor.

Electrokinetic stringency control for single-base mismatch detection

To optimize the ability of electrokinetics to improve the specificity of the electrochemical biosensor, electrokinetic stringency control was characterized using synthetic targets, including a perfect match sequence and a single-base mismatch sequence. The voltage dependences of the signal for different targets were obtained (Figure 2). The values were normalized by the signal of the perfect match target at room temperature. For the

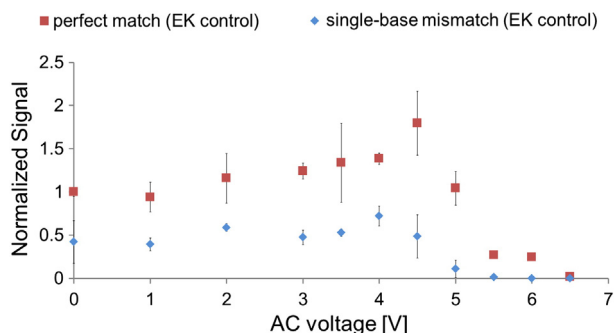


Figure 2. Fraction of species (perfect match and single-base mismatch) by applying a 200 kHz square wave. The signal was normalized by the signal of the perfect match target at room temperature.

perfect match target, the signal increased at low voltage and reached a peak value at voltage of 4.5 Vpp. Further increase in the applied voltage was observed to reduce the signal. The mismatch target displayed a similar trend, but had a lower value of the peak voltage at 4 Vpp. In general, the perfect match target had a higher signal compared to the mismatch target. The signals between the perfect match and single-base mismatch targets were clearly distinguished with an applied voltage between 5 and 6 Vpp.

To further analyze the contribution of Joule heating and electrothermal flow, the temperature was measured at different applied voltages and the hybridized fraction was determined under different conditions (Figure 3, A). The theoretical melting curves of the two targets were calculated based on the nearest-neighbor model to compare to the experimental results (Figure 3, B). In addition, the experiment was performed using an incubator with temperature control to elucidate the effects of electrothermal flow in electrokinetic stringency control (Figure 3, C). The melting curves obtained from the incubator are in reasonable agreement with the theoretical model. In particular, the theoretical model correctly predicted the melting temperatures for both the perfect match and mismatch targets. In this study, the melting temperature is considered the temperature at which 50% of the maximum signal is obtained. Remarkably, the maximum signal obtained by electrokinetic stringency control was significantly higher than the value obtained by the incubator. The melting curve obtained with electrokinetics shifted to a lower temperature compared to the one obtained by the incubator. Furthermore, the melting curve of the perfect match target was at a higher temperature range compared to the melting curve of the mismatch target.

Electrokinetic stringency control can be understood by a combination of temperature elevation and electrothermal fluid motion. At room temperature, the perfect match and single-base mismatch targets can hybridize with the capture and detector probes. The difference between the perfect match and mismatch targets is primarily due to the differences in the target sequences and binding affinities of the targets to the capture probe. With electrokinetics, the temperature increases with voltage and follows a second-power dependence.³¹ The signal, in particular for the perfect match target, displays a significant enhancement, one that is higher than the value obtained using the incubator. The enhancement is the result of the electrothermal flow that assists

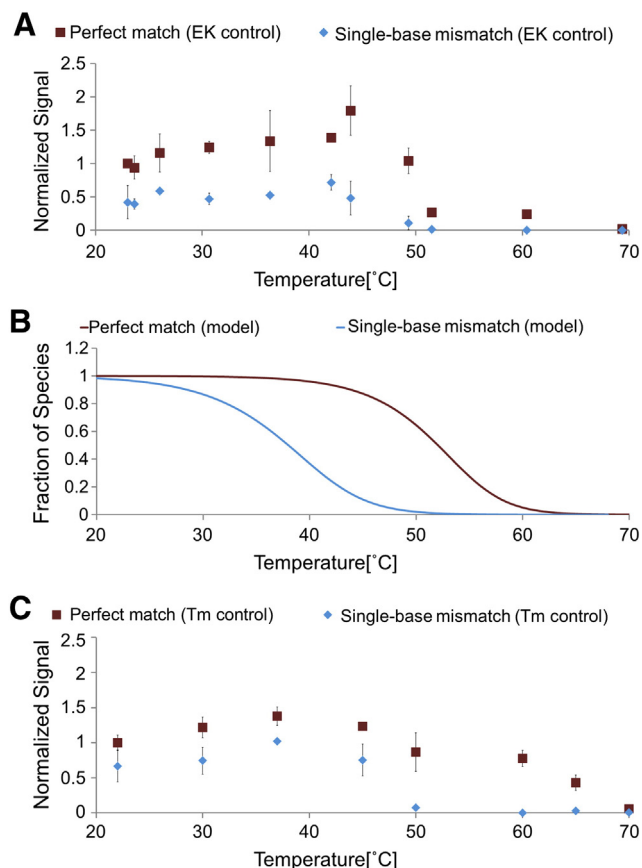


Figure 3. Comparison of (A) experimental fraction (perfect match and single-base mismatch) results with different temperatures driven by electrokinetics, (B) predicted fraction (perfect match and single-base mismatch) of nearest-neighbor model and (C) experimental fraction results in temperature control with an incubator.

molecular transportation and of the temperature rise that facilitates nucleic acid hybridization.¹² It should be noted that the effect of fluid advection is not considered in the theoretical model. Since the mismatch target has a lower affinity, it has a lower melting temperature, as observed in the experiment. At a higher temperature, the signal decreases with the voltage due to the disassociation of the target from the capture probe. An interesting observation is that the melting temperatures with electrokinetics are lower than the values predicted by the theoretical model and obtained using the incubator. Under the same temperature, the deviation in melting curves cannot be explained by thermal denaturation and suggests the significance of the electrothermal flow motion in electrokinetic stringency control. In particular, the electrothermal fluid motion serves as stringency wash for removing non-specific binding. These results reveal that electrokinetic stringency control can improve the specificity of the assay for single nucleotide mismatch detection, which forms the foundation for multiplex electrochemical pathogen sensing toward urinary tract infection diagnosis.

Electrokinetic stringency control for matrix effect

Urine samples contain various components contributing toward the matrix effect, which influences the performance of

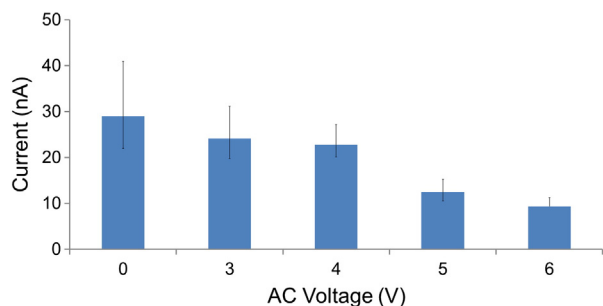


Figure 4. Voltage dependence of the background noise in human urine samples.

the electrochemical sensor. The concentrations of the matrix components can vary depending on diet and liquid intake by the patient.¹⁵ For the electrochemical sensor, a strong matrix effect may reduce the signal-to-noise ratio and the detection limit of the assay. By applying an electric field, a strong electrothermal flow and large temperature rise can be induced to increase the stringency for surface binding and remove the non-specific binding caused by the interaction between matrix components and the sensor surface. Therefore, we examined the ability of electrokinetic stringency control to reduce the background noise of urine samples from healthy human volunteers (Figure 4). In the experiment, it was observed that both the background levels and their standard deviation decrease with the applied voltage. The background noise could be reduced by 60% with 6 Vpp. The data demonstrate that electrokinetic stringency control can reduce the interference of the matrix effect on the electrochemical sensor and potentially improve the reliable of the assay.

Electrokinetic stringency control for multiplex pathogen detection

Crosstalk between different sensors can be a challenge for multiplex pathogen detection. Crosstalk may arise from the association of co-infections of pathogens that have similar 16S rRNA sequences or non-specific binding between the capture and detector probes. In general, a specific pair of capture and detector probes can be designed for each bacterial species without crosstalk. Nevertheless, the sequence design could be challenging when multiple detector probes (i.e., the cocktail approach) are applied simultaneously for multiplex detection. While the detector probes may have a low binding affinity with the capture probes, a high concentration of detector probes can still increase the background noise. Therefore, we explored electrokinetic stringency control for eliminating the crosstalk for multiplex detection. Bacterial lysates with the detector probe cocktails were loaded to sensor capture probes for *E. coli*, *P. mirabilis*, and *P. aeruginosa* pre-coated on the sensor surfaces. *P. mirabilis* and *P. aeruginosa* have similar sequences with *E. coli* in the capture probe binding domain.³⁹ Figure 5 shows the amperometric signals with and without electrokinetic control. Without electrokinetics, a significant false positive was observed at room temperature for the *E. coli* sensor with *P. mirabilis* and *P. aeruginosa*. Significant background noise was also observed between the *E. coli* capture probe and the detector probe cocktail

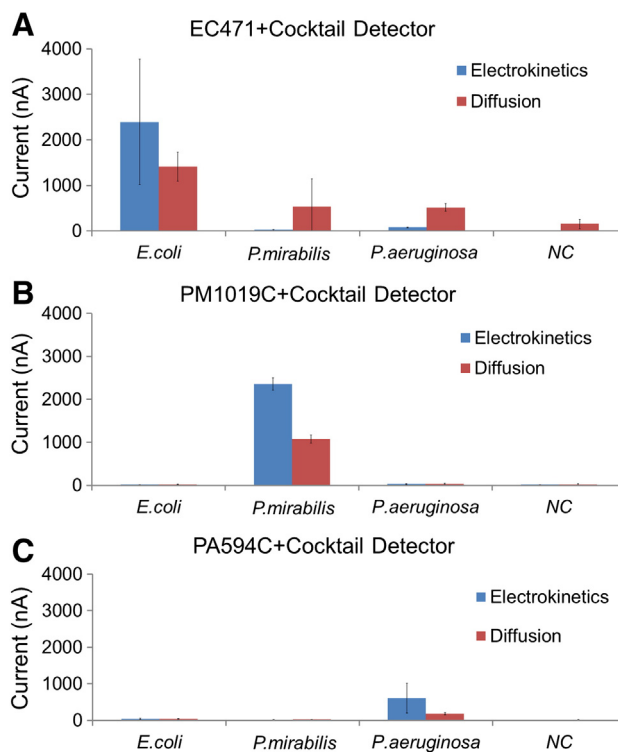


Figure 5. Multiplex detection of bacterial clinical isolates (*P. mirabilis* 1.11×10^7 CFU/ml, *P. aeruginosa* 1.0×10^7 CFU/ml, *E. coli* 3.2×10^6 CFU/ml) using (A) *E. coli* capture probe, (B) *P. mirabilis* capture probe and (C) *P. aeruginosa* capture probe and cocktail detector probe with and without *in situ* electrokinetic stringency control.

(negative control in Figure 5, A). A voltage of 6 Vpp was selected in the electrokinetic experiment where the hybridization buffer reached ~ 60 °C. This temperature is below the melting temperature of *E. coli*, but it exceeds the melting temperature of *P. aeruginosa* and *P. mirabilis*. With electrokinetic stringency control, the amperometric signal of *E. coli* in the *E. coli* sensor (EC 471C) was increased by 2-fold, and the background noise (NC) was decreased more than 10-fold. At the same time, the crosstalk generated by *P. aeruginosa* and *P. mirabilis* was reduced to a level similar to the negative control. Applying *in situ* electrokinetic stringency control enhanced the signal-to-noise ratio for *E. coli* more than 20-fold while also significantly reducing the false positives from *P. mirabilis* and *P. aeruginosa*. In the *P. mirabilis* and *P. aeruginosa* sensors, the target signals were increased in electrokinetic control, and background noise levels (negative control) were decreased. Collectively, our results demonstrate *in situ* electrokinetic stringency control can significantly improve the performance of the SAM-based biosensor array for multiplex detection of uropathogens.

Discussion

In this study, we demonstrated an *in situ* electrokinetic stringency control technique for enhancing the specificity of a SAM-based electrochemical nucleic acid biosensor. Our results

showed AC electrokinetic stringency control has the ability to reduce matrix effects and background noise. Synthetic targets and uropathogenic clinical isolates were tested and studied under different AC electrokinetic conditions. The results of single-base mismatch detection reveal that electrokinetics can create a controllable temperature rise and electrothermal fluid flow to remove non-specific binding. Electrokinetic stringency control also successfully eliminated the false positives in multiplex detection and increased the signal-to-noise ratio over 20-fold. These promising results enable new opportunities for electrokinetic stringency control to address the challenges of integrated biosensing systems for point-of-care diagnostics of UTI and other infectious diseases. Compared to standard stringency control strategies, such as temperature elevation, the electrothermal fluid motion allows effective transportation of target molecules and non-specific binding removal, which increases the overall signal-to-noise ratio. Furthermore, electrokinetic stringency control is particular suitable for point-of-care diagnostics, since only electronic interfaces are required to implement the electrokinetic enhanced SAM-based electrochemical molecular biosensors.

In conclusion, electrochemical sensing is an efficient platform toward a wide spectrum of point-of-care diagnostic applications. A major barrier toward clinical translation of a biosensor is the matrix effect of physiological samples, which introduce significant background noise and non-specific binding. The matrix effect hinders the translation of many biosensing platforms from proof-of-concept stage to clinical adoption. With an in situ electrokinetic stringency control technique, we demonstrate a SAM-based electrochemical biosensor enables specific multiplex urinary tract infection diagnosis by removing non-specific binding and matrix effects. Since non-specific binding and matrix effects represent fundamental obstacles in various bioassays, electrokinetic stringency control is anticipated to benefit a large number of biomedical applications in the future.

References

- Mach KE, Wong PK, Liao JC. Biosensor diagnosis of urinary tract infections: a path to better treatment? *Trends Pharmacol Sci* 2011;**32**:330-6.
- Griebing TL. Urologic diseases in america project trends in resource use for urinary tract infections in women. *J Urol* 2005;**173**:1281-7.
- Griebing TL. Urologic diseases in america project: trends in resource use for urinary tract infections in men. *J Urol* 2005;**173**:1288-94.
- Sin ML, Gao J, Liao JC, Wong PK. System integration - a major step toward lab on a chip. *J Biol Eng* 2011;**5**:6.
- Choi S, Goryll M, Sin MLY, Wong PK, Chae J. Microfluidic-based biosensors toward point-of-care detection of nucleic acids and proteins. *Microfluidics Nanofluidics* 2011;**10**:231-47.
- Liu RH, Yang JN, Lenigk R, Bonanno J, Grodzinski P. Self-contained, fully integrated biochip for sample preparation, polymerase chain reaction amplification, and DNA microarray detection. *Anal Chem* 2004;**76**:1824-31.
- Pan Y, Sonn GA, Sin MLY, Mach KE, Shih MC, Gau V, et al. Electrochemical immunosensor detection of urinary lactoferrin in clinical samples for urinary tract infection diagnosis. *Biosens Bioelectron* 2010;**26**:649-54.
- Mach KE, Du CB, Phull H, Haake DA, Shih MC, Baron EJ, et al. Multiplex pathogen identification for polymicrobial urinary tract infections using biosensor technology: a prospective clinical study. *J Urol* 2009;**182**:2735-41.
- Gabig-Ciminska M. Developing nucleic acid-based electrical detection systems. *Microb Cell Fact* 2006;**5**.
- Wang J. From DNA, biosensors to gene chips. *Nucleic Acids Res* 2000;**28**:3011-6.
- Mohan R, Mach KE, Bercovici M, Pan Y, Dhulipala L, Wong PK, et al. Clinical validation of integrated nucleic acid and protein detection on an electrochemical biosensor array for urinary tract infection diagnosis. *PLoS One* 2011;**6**:e26846.
- Sin MLY, Liu TT, Pyne JD, Gau V, Liao JC, Wong PK. In situ electrokinetic enhancement for self-assembled-monolayer-based electrochemical biosensing. *Anal Chem* 2012;**84**:2702-7.
- Liao JC, Mastali M, Gau V, Suchard MA, Moller AK, Bruckner DA, et al. Use of electrochemical DNA biosensors for rapid molecular identification of uropathogens in clinical urine specimens. *J Clin Microbiol* 2006;**44**:561-70.
- Gau V, Ma SC, Wang H, Tsukuda J, Kibler J, Haake DA. Electrochemical molecular analysis without nucleic acid amplification. *Methods* 2005;**37**:73-83.
- Chiu ML, Lawi W, Snyder ST, Wong PK, Liao JC, Gau V. Matrix effect - a challenge toward automation of molecular analysis. *J Assoc Lab Automation* 2010;**15**:233-42.
- Call DR. Challenges and opportunities for pathogen detection using DNA microarrays. *Crit Rev Microbiol* 2005;**31**:91-9.
- Lagally ET, Scherer JR, Blazej RG, Toriello NM, Diep BA, Ramchandani M, et al. Integrated portable genetic analysis microsystem for pathogen/infectious disease detection. *Anal Chem* 2004;**76**:3162-70.
- Elnifro EM, Ashshi AM, Cooper RJ, Klapper PE. Multiplex PCR: optimization and application in diagnostic virology. *Clin Microbiol Rev* 2000;**13**:559-70.
- Heller MJ, Forster AH, Tu E. Active microelectronic chip devices which utilize controlled electrophoretic fields for multiplex DNA hybridization and other genomic applications. *Electrophoresis* 2000;**21**:157-64.
- Matte-Tailliez O, Quence P, Cibik R, van Opstal J, Dessevre F, Firmesse O, et al. Detection and identification of lactic acid bacteria in milk and industrial starter culture with fluorescently labeled rRNA-targeted peptide nucleic acid probes. *Lait* 2001;**81**:237-48.
- Bourne DG, Holmes AJ, Iversen N, Murrell JC. Fluorescent oligonucleotide rDNA probes for specific detection of methane oxidising bacteria. *FEMS Microbiol Ecol* 2000;**31**:29-38.
- Takeda T, Peina Y, Ogawa A, Dohi S, Abe H, Nair GB, et al. Detection of heat-stable enterotoxin in a cholera-toxin gene-positive strain of vibrio-cholerae-o1. *FEMS Microbiol Lett* 1991;**80**:23-7.
- Henderson GS, Conary JT, Davidson JM, Stewart SJ, House FS, Mccurley TL. A reliable method for northern blot analysis using synthetic oligonucleotide probes. *Biotechniques* 1991;**10**:190-7.
- Trebesius K, Panthel K, Strobel S, Vogt K, Faller G, Kirchner T, et al. Rapid and specific detection of helicobacter pylori macrolide resistance in gastric tissue by fluorescent in situ hybridisation. *Gut* 2000;**46**:608-14.
- Sosnowski RG, Tu E, Butler WF, O'Connell JP, Heller MJ. Rapid determination of mismatch mutations in DNA hybrids by direct electric field control. *Proc Natl Acad Sci USA* 1997;**94**:1119-23.
- Strachan T, Read AP. *Human molecular genetics. 2nd ed.* New York. Chichester England: Wiley-Liss; 1999.
- Wong PK, Wang TH, Deval JH, Ho CM. Electrokinetics in micro devices for biotechnology applications. *IEEE-ASME Transactions on Mechatronics* 2004;**9**:366-76.
- Erickson D, Liu XZ, Venditti R, Li DQ, Krull UJ. Electrokinetically based approach for single-nucleotide polymorphism discrimination using a microfluidic device. *Anal Chem* 2005;**77**:4000-7.

29. Green NG, Ramos A, Gonzalez A, Castellanos A, Morgan H. Electrothermally induced fluid flow on microelectrodes. *J Electrostatics* 2001;**53**:71-87.
30. Castellanos A, Ramos A, Gonzalez A, Green NG, Morgan H. Electrohydrodynamics and dielectrophoresis in microsystems: scaling laws. *J Phys D: Appl Phys* 2003;**36**:2584-97.
31. Ramos A, Morgan H, Green NG, Castellanos A. Ac electrokinetics: a review of forces in microelectrode structures. *J Phys D: Appl Phys* 1998;**31**:2338-53.
32. Sin MLY, Gau V, Liao JC, Wong PK. Electrothermal fluid manipulation of high-conductivity samples for laboratory automation applications. *J Assoc Lab Automation* 2010;**15**:426-32.
33. Heller MJ. An active microelectronics device for multiplex DNA analysis. *IEEE Eng Med Biol Mag* 1996;**15**:100-4.
34. Erickson D, Liu XZ, Krull U, Li DQ. Electrokinetically controlled DNA hybridization microfluidic chip enabling rapid target analysis. *Anal Chem* 2004;**76**:7269-77.
35. Ross D, Gaitan M, Locascio LE. Temperature measurement in microfluidic systems using a temperature-dependent fluorescent dye. *Anal Chem* 2001;**73**:4117-23.
36. Sakakibara J, Adrian RJ. Whole field measurement of temperature in water using two-color laser induced fluorescence (vol 26, pg 7, 1999). *Experiments in Fluids* 1999;**27**:U1.
37. SantaLucia J. A unified view of polymer, dumbbell, and oligonucleotide DNA nearest-neighbor thermodynamics. *Proc Natl Acad Sci USA* 1998;**95**:1460-5.
38. Leber M, Kaderali L, Schonhuth A, Schrader R. A fractional programming approach to efficient DNA melting temperature calculation. *Bioinformatics* 2005;**21**:2375-82.
39. Cole JR, Wang Q, Cardenas E, Fish J, Chai B, Farris RJ, et al. The ribosomal database project: improved alignments and new tools for rRNA analysis. *Nucleic Acids Res* 2009;**37**:D141-5.